Implications of cross-species interactions on the temperature dependence of Kapitza conductance

John C. Duda, Timothy S. English, Edward S. Piekos, William A. Soffa, Leonid V. Zhigilei, and Patrick E. Hopkins

Phys. Rev. B **84**, 193301 — Published 8 November 2011

DOI: 10.1103/PhysRevB.84.193301

Implications of cross-species interactions on the temperature dependence of Kapitza conductance

John C. Duda,[1,2,*] Timothy S. English,[2,3] Edward S. Piekos,[2] William A. Soffa,[4] Leonid V. Zhigilei,[4] and Patrick E. Hopkins[1,†]

[1]*Department of Mechanical and Aerospace Engineering, University of Virginia, Charlottesville, Virginia 22904*
[2]*Sandia National Laboratories, Albuquerque, New Mexico 87185*
[3]*Department of Mechanical Engineering, Stanford University, Stanford, California 94305*
[4]*Department of Materials Science and Engineering, University of Virginia, Charlottesville, Virginia 22904*

(Dated: October 21, 2011)

We investigate the behavior of Kapitza conductance at interfaces between two Lennard-Jones fcc solids as a function of the range and strength of cross-species interactions via molecular dynamics simulations. It is found that decreasing either of these quantities leads to a reduction in the slope of linear temperature dependence of Kapitza conductance, suggesting a corresponding decrease in the probability of inelastic phonon-phonon interactions. To further explore the mechanisms responsible for such behavior, we calculate the phonon density of states and spectral temperature of each of the monolayers adjacent to the interface. It is found that the reduction of the range and strength of cross-species interactions leads to a softening of the density of states near the interface, while the spectral temperature calculations provide further evidence that such reductions decrease the probability of inelastic phonon scattering. These findings help explain varying accounts of the temperature dependence of Kapitza conductance observed in previous works.

PACS numbers: 63.22.-m, 65.40.-b, 66.70.-f

TABLE I. Cross-species interactions for each sample, as well as the slopes and 0 K extrapolations (y-intercepts) of the linear fits to the h_K data. While the slopes vary by a factor of two, the 0 K extrapolations are within 10 % of each other. Note that sample VI is used only to study the vibrational characteristics of free surfaces and not h_K.

Sample	r_c (σ)	ε_{AB} (ε)	Slope ($\mathrm{MW\,m^{-2}\,K^{-2}}$)	0 K Extrapolation ($\mathrm{MW\,m^{-2}\,K^{-1}}$)
I	2.50	1.0	2.29	25.2
II	2.30	1.0	2.09	25.1
III	2.05	1.0	2.01	24.6
IV	1.75	1.0	1.60	24.5
V	1.35	1.0	1.27	23.1
VI	0.00	0.0	-	-
VII	2.50	0.5	1.07	23.6

Thermal transport in nanostructured materials differs from that in bulk due to the high density of interfaces within them. Consequently, many experimental,[1,2] computational,[3–10] and empirical[11,12] approaches have sought to investigate and explain the behavior of thermal transport across interfaces, the efficiency of which can be described by the Kapitza conductance of the interface, or h_K.[13] Semiconductor systems are a primary focus due to their widespread integration in electronic and optical devices. In semiconductors, a majority of the heat is carried by phonons. As a result, classical molecular dynamics simulations are well suited to study thermal transport across interfaces within such systems, as the time-evolution of the positions and energies of atoms around an interface are exactly known. More specifically, non-equilibrium molecular dynamics (NEMD) simulations have been routinely employed to study h_K.[3–10] In a NEMD simulation, a thermal flux, Q, is applied across a computational domain containing the interface of interest. Consequently, spatial temperature gradients develop in the materials comprising the interface, while a temperature discontinuity develops at the interface between them. This discontinuity, ΔT, can be related to h_K through the relationship $Q = h_K \Delta T$.

One critical parameter affecting the magnitude of h_K is the "strength" of interactions between the materials comprising the interface, as has been demonstrated in several previous NEMD studies.[5–7] However, these studies have been limited to Si-α:polyethylene (Ref. 5) and carbon-nanotube:SiO_2 (Ref. 6) solid-solid interfaces and Lennard-Jones (LJ) type solid-liquid interfaces (Ref. 7). Consequently, results varied due to differences in parameterization across these studies. In the present work, we seek to generalize this interface-bonding condition by investigating the behavior of h_K at interfaces between two LJ fcc solids as a function of temperature with varying cross-species interactions (i.e., A-B interactions) via NEMD simulations. We quantify these cross-species interactions by means of both their range (or cutoff radius, $r_{c,AB}$) *and* strength (ε_{AB}) relative to that of interactions between atoms of the same type (i.e., A-A or B-B interactions).

All computational cells were $8 \times 8 \times 80$ conventional unit cells in size and contained 20,480 atoms; one half of the atoms were A-type and the other half were B-type, separated by an interface at the midpoint of the computational cell in the z-direction. A- and B-type atoms were distinguished by their masses alone (40 and 120 amu, respectively). All interactions were described by the 6-12 LJ potential, $U(r) = 4\varepsilon\left[(\sigma/r)^{12} - (\sigma/r)^{6}\right]$, where r is the interatomic separation and σ and ε are the LJ length and energy parameters. For A-A and B-B interactions, the potential was parameterized for Ar,[14] where $\sigma = 3.37\,\text{Å}$ and $\varepsilon = 0.0103\,\text{eV}$. The cutoff distance (radius beyond which the potential was truncated and $U = 0$) was set to $r_c = 2.5\sigma$. Cross-species interactions, $r_{c,AB}$ and ε_{AB}, were varied from system to system and are described in terms of σ and ε. The values selected for $r_{c,AB}$ correspond to radii between concentric nearest-neighbor shells.[15] The cross-species interaction parameters for each of the seven samples considered are summarized in Table I.

In all samples, the four outermost monolayers in the z-direction formed a rigid wall. The eight monolayers immediately inside these walls were bath atoms, to which energy could be added or removed to establish a temperature gradient. During the simulation, the equations of motion for the system were integrated using the Nordsieck fifth-order predictor corrector algorithm[16] with a time step of 4.28 fs. The systems were equilibrated at a predefined temperature via a velocity scaling routine and zero pressure, maintained by the Berendsen barostat algorithm.[17] In this routine, pressure is calculated for all dynamic atoms and the volume scaling involved displacement of the rigid walls. Once equilibration was complete, velocity-fluctuation time series were generated for computation of the local phonon density of states (DOS) and equilibrium thermal energy spectra (or TES, a measure of the phononic thermal energy per unit frequency).[9,21,22] Subsequently, the NEMD procedure was implemented. The addition of energy to/removal from the baths was performed through a constant-flux approach;[18,19] for h_K calculations $Q = 0.54\,\mathrm{MW\,m^{-2}}$. During NEMD, the systems were divided into 160 equally sized bins such that spatial temperature profiles could be calculated along the z-axis. Once in steady-state, time-averaged profiles were constructed from 3,000 system snapshots taken over 1.5×10^6 time steps (6.42 ns). A linear least-squares fit was then performed for each half of the domain. The eight bins nearest to the bath and the interface were not included in these fits. The discontinuity between the fits at the interface was

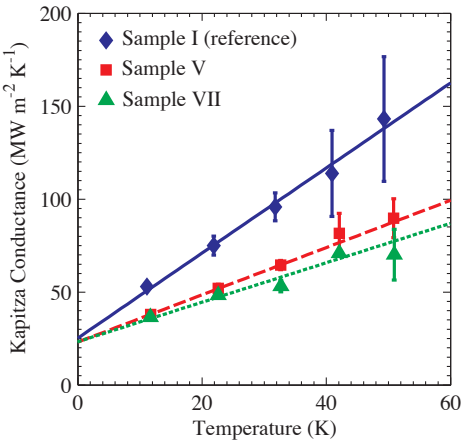

FIG. 1. Temperature-dependent h_K data from NEMD simulations for samples I, V, and VII. Each data point is the averaged over three to five independent simulations and error bars represent the standard deviation, i.e., repeatability. Solid and dashed lines are linear fits of the data. While the slopes of these linear fits exhibit strong dependence on cross-species interaction parameters, the y-intercepts do not.

used to calculate h_K. With flux still applied, additional velocity-fluctuation time series were generated for computation of the TES during NEMD.

To investigate the role of cross-species interactions on thermal transport across interfaces, we have calculated h_K for different values of $r_{c,AB}$ and ε_{AB}. Figure 1 shows h_K as a function of T for samples I, V, and VII, where sample I serves as a reference ($r_{c,AB} = r_c$ and $\varepsilon_{AB} = \varepsilon$), while sample V has a shorter cross-species interaction range and sample VII has weaker cross-species interactions. For each combination of parameters the data demonstrate a linear dependence of h_K on T. This linear dependence has been attributed to an increase in inelastic phonon scattering at the interface with increasing T due to the corresponding increase in phonon population.[3,4] However, as either $r_{c,AB}$ or ε_{AB} decrease, this dependence is less pronounced, suggesting that inelastic phonon scattering is inhibited as the interactions between the solids comprising the interface are themselves limited. In addition, the data indicate that h_K becomes less sensitive to the cross-species interaction parameters as T goes to zero. Furthermore, it is interesting to note that extrapolation of these linear trends to 0 K yields a nearly constant y-intercept, suggesting that h_K can be considered a superposition of temperature-dependent and independent processes. Such a description is consistent with the concepts outlined in our previous work.[20] A summary of the results obtained with different cross-species interaction parameters is presented in Table I.

To further explore the mechanisms responsible for this observed behavior, we calculated the local phonon DOS and spectral temperature of each of the monolayers adjacent to the interface. The DOS within the few monolayers near the interface should differ from that of either bulk material A or B due to the presence of the interface. In order to quantify this difference, we have calculated the DOS, $D(\omega)$, of both monolayers adjacent to the interface, as well as that of bulk material A and B. The DOS is proportional to the Fourier transform ($\mathscr{F}$) of the velocity correlation function (VACF)[16] but in practice is calculated using standard estimation procedures for power spectral density. Within each monolayer of interest, the velocity of 20 atoms is obtained at each integration time step to give a velocity fluctuation time series of 73,728 points. The Welch method of power spectral density estimation is then applied by creating eight 50 % overlapping segments of 16,384 points to give an angular frequency resolution of 8.96×10^{10} rad s^{-1} based on our time step of 4.428 fs. Each segment is then multiplied by a Hamming window and the fast Fourier transform is computed. The power spectral density, equivalent to $\mathscr{F}$(VACF), is then obtained by ensemble averaging the Fourier transform magnitudes of each segment. In order to compute the DOS in units of counts per frequency per volume, $\mathscr{F}$(VACF) must be further normalized as follows:

$$D(\omega) = \frac{1}{2} m \mathscr{F}\left(\text{VACF}\right) \frac{1}{k_B T} \rho, \tag{1}$$

where m is the atomic mass, k_B is the Boltzmann constant, T is the local temperature, and ρ is the atomic density.

Figure 2 shows the calculated DOS for bulk materials A and B and the monolayers immediately adjacent to the interface for different values of $r_{c,AB}$ and ε_{AB}. It is clear that a reduction in either $r_{c,AB}$ (sample V) or ε_{AB} (sample VII) causes a softening of modes on both sides of the interface, as evidenced by a depletion of high frequency modes and enhancement of low frequency modes as compared to the reference (sample I). The larger the reduction in either range or strength of cross-species interactions, the greater the softening. This can be attributed to the fact that as $r_{c,AB}$ and ε_{AB} go to zero, the interface tends toward the limit where the monolayers adjacent to the interface are non-interacting free surfaces (sample VI). It is also interesting to note that

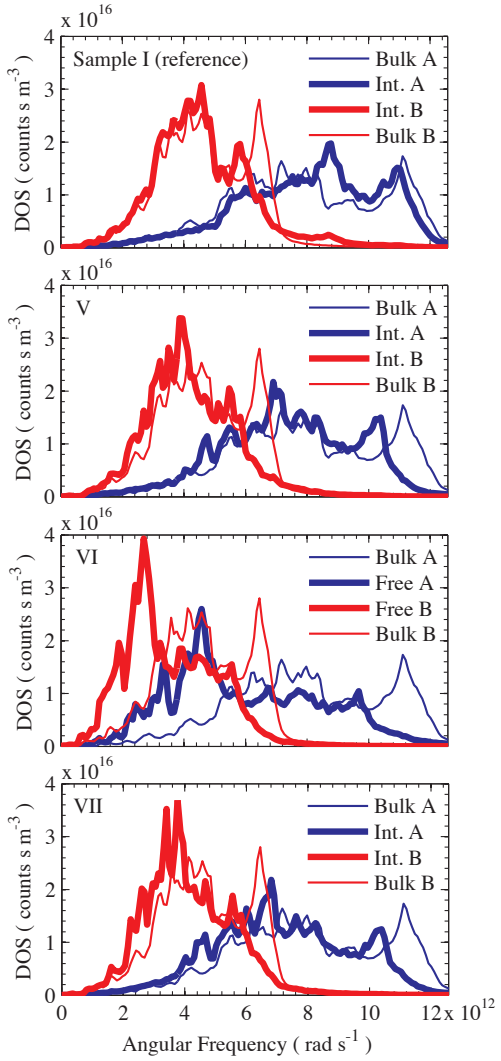

FIG. 2. (Color online) Phonon density of states curves at 12 K calculated via Eq. 2 within the monolayers adjacent to the interface (heavy lines) compared to bulk (light lines). A reduction in either $r_{c,\mathrm{AB}}$ or $\varepsilon_{\mathrm{AB}}$ causes a softening of modes on both sides of the interface.

through visual inspection of Fig. 2, the degree of softening at the interface in samples V and VII is nearly the same, as were the calculated values of h_{K} at the same simulation temperature (12 K, see Fig. 1). This suggests that reductions in either the range or strength of cross-species interactions at the interface can have similar effects on the vibrational and thermal properties of the interface. That is, if the vibrational properties of the interface are similar, the thermal behavior can be expected to be similar as well, even if the cause for this vibrational similarity is unique to each sample.

The vibrational spectra of the monolayer within material A adjacent to the interface can lend further insight into thermal transport across an interface by way of using them as a means of establishing a spectrally-resolved temperature, $T(\omega)$.[9,21,22] Knowledge of $T(\omega)$ can provide insight into the strength of coupling of vibrational modes between two bodies at different temperatures. Furthermore, spectrally resolving the temperature near the interface will indicate if elastic phonon scattering dominates, or if inelastic scattering offers another channel for heat to flow across the interface. In the case of elastic scattering, temperature will be spectrally dependent near the interface since only the "elastically accessible" modes will be heated or cooled by the other material comprising the interface. On the other hand, if inelastic scattering provides an alternative channel across the interface, there will be no spectral temperature dependence. In order to calculate $T(\omega)$, we first calculate the thermal energy spectrum, $g(\omega)$, of the monolayer within material A adjacent to the interface when the system is both in an equilibrium state and when the system is subject to a steady-state flux as per the NEMD routine; we refer to these quantities as $g_{eq}(\omega)$ and $g_{ss}(\omega)$, respectively. The thermal energy spectrum in units of energy per frequency per volume is related to the phonon DOS and is

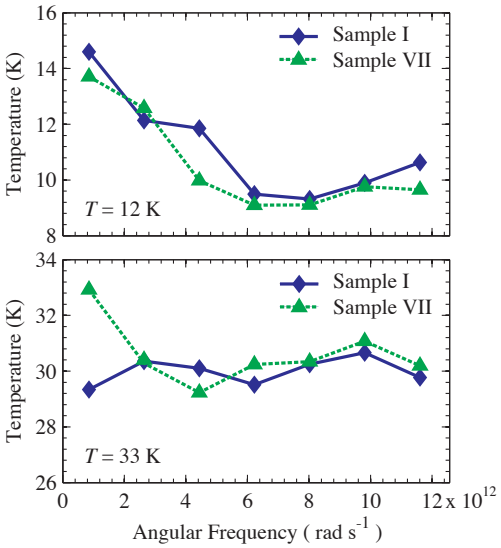

FIG. 3. (Color online) Spectral temperature of the monolayer within material A adjacent to the interface for two different cross-species interactions at average interface temperatures of (a) 12 K and (b) 33 K. The "flatness" of these curves is indicative of the means of energy transfer across the interface, i.e., elastic-only or elastic and inelastic. At 12 K, the spectral-temperature dependence suggests elastic scattering dominates at both interfaces. At 33 K, only the weakly-bonded interface exhibits spectral temperature dependence, suggesting that inelastic channels are inhibited in systems where the interface is poorly bonded. The absolute values of $T(\omega)$ are not indicative of the strength of coupling, as the average interface temperature varied slightly from simulation to simulation.

given as

$$g(\omega) = \frac{1}{2} m \mathscr{F}\left(\mathrm{VACF}(t)\right) \rho. \tag{2}$$

Subsequently, $T(\omega)$ can then be defined as

$$T(\omega) = T_{eq} \frac{g_{ss}(\omega)}{g_{eq}(\omega)}, \tag{3}$$

where T_{eq} is the temperature at equilibrium. In order to more clearly resolve $T(\omega)$, we increased Q by a factor of three ($1.63\,\mathrm{MW\,m^{-2}}$). When performing further h_{K} calculations, we found this change in Q did not affect our results.

Figure 3 shows the spectral temperature of the monolayer within material A adjacent to the interface in samples I and VII (the reference sample and a sample with a weakly bonded interface, respectively) at average interface temperatures 12 and 33 K. During the NEMD simulations, the cold bath is at the end of material A, while the hot bath is at the end of material B. Consequently, the monolayer within material A adjacent to the interface is at a lower spectrally-averaged temperature than the monolayer within material B adjacent to the interface. However, when the temperature of the monolayer within material A adjacent to the interface is resolved spectrally at an average interface temperature of 12 K, it is clear that low frequency modes are at noticeably higher temperatures than high frequency modes. This indicates that the low frequency modes are better coupled to the hotter material B than the high frequency modes. In fact, the modes which are hotter in the monolayer within material A adjacent to the interface are those that fall below the maximum frequency of material B ($\approx 7 \times 10^{12}\,\mathrm{rad\,s^{-1}}$), indicating that at low temperatures, thermal transport across the interface is dominated by elastic phonon-phonon interactions. At this temperature, the differences in bonding at the interface between samples I and VII have little impact on $T(\omega)$. On the other hand, when the temperature of the monolayer within material A adjacent to the interface is resolved spectrally at an average interface temperature of 33 K, sample I shows no frequency dependence, whereas sample VII still exhibits frequency dependence (albeit this dependence is slightly diminished when compared to that at 12 K). In sample I, the lack of frequency dependence of $T(\omega)$ indicates that inelastic phonon scattering is contributing to thermal transport across the interface, e.g., $\omega_{1,\mathrm{B}} + \omega_{2,\mathrm{B}} \rightarrow \omega_{3,\mathrm{A}}$, where $\omega_{3,\mathrm{A}}$ is a frequency greater than the maximum frequency of material B. In contrast, the temperature near the weakly-bonded interface (sample VII) exhibits frequency dependence. This suggests that the strength of inelastic scattering, which generally increases with temperature, may be limited due to interface conditions, e.g., reduced strength or range of bonding interactions (an alternative expression of this concept is that changes in interface bonding change intrinsic scattering rates in the

material immediately adjacent to the interface). This is consistent with the results plotted in Fig. 1, where the linear dependence of h_K on T is much less pronounced for the weakly-bonded interface as compared to the reference system.

In conclusion, we have demonstrated that the conditions of the interface, controlled in this work by either the range or strength of cross-species interactions, can have a significant impact on the temperature dependence of h_K, even for atomically perfect interfaces. Interfaces characterized by short-range or weak cross-species interactions can exhibit surface-like phonon density of states near the interface. In addition, the temperature dependence of h_K may not be as pronounced for such interfaces. Spectral temperature analysis suggests this is the direct result of inhibited inelastic phonon-phonon interactions at weakly bonded interfaces. This parameterization can lend further insight into the results of previous MD studies. For example, in two recent studies examining h_K between solids and alkanedithiol-based self-assembled-monolayers,[8,10] one demonstrated temperature dependence of h_K[8] while the other did not.[10] However, the interface bond strength was ≈ 7.5 times greater in the study exhibiting the linear temperature dependence, where our results suggest that stronger bonding supported greater inelastic scattering at the interface. Thus, these prior studies are consistent with the above findings and emphasize the role of interface conditions on inelastic scattering and the temperature dependence of Kapitza conductance.

J.C.D. and T.S.E. are appreciative for funding from the National Science Foundation through the Graduate Research Fellowship Program. The authors at Sandia National Laboratories acknowledge funding from the LDRD program office. T.S.E. is appreciative for support from the Department of Defense through the National Defense Science & Engineering Graduate Fellowship Program. L.V.Z. acknowledges funding from the National Science Foundation (CBET-1033919). Sandia National Laboratories is a multiprogram laboratory managed and operated by Sandia Corporation, a wholly owned subsidiary of Lockheed Martin Corporation, for the United States Department of Energy's National Nuclear Security Administration under Contract DE-AC04-94AL85000.

* duda@virginia.edu
† phopkins@virginia.edu

[1] D. G. Cahill, W. K. Ford, K. E. Goodson, G. D. Mahan, A. Majumdar, H. J. Maris, R. Merlin, and S. R. Phillpot, Journal of Applied Physics **93**, 793 (2003).
[2] P. M. Norris and P. E. Hopkins, Journal of Heat Transfer **131**, 043207 (2009).
[3] R. J. Stevens, L. V. Zhigilei, and P. M. Norris, International Journal of Heat and Mass Transfer **50**, 3977 (2007).
[4] E. S. Landry and A. J. H. McGaughey, Physical Review B **80**, 165304 (2009).
[5] M. Hu, P. Keblinski, and P. K. Schelling, Physical Review B **79**, 104305 (2009).
[6] Z.-Y. Ong and E. Pop, Physical Review B **81**, 155408 (2010).
[7] Y. Wang and P. Keblinski, Applied Physics Letters **99**, 073112 (2011).
[8] T. Luo and J. R. Lloyd, Journal of Applied Physics **109**, 034301 (2011).
[9] L. Hu, T. Desai, and P. Keblinski, Physical Review B **83**, 195423 (2011).
[10] T. Luo and J. R. Lloyd, Journal of Heat Transfer **132**, 032401 (2010).
[11] W. A. Little, Canadian Journal of Physics **37**, 334 (1959).
[12] E. T. Swartz and R. O. Pohl, Reviews of Modern Physics **61**, 605 (1989).
[13] P. L. Kapitza, Physical Review **60**, 354 (1941).
[14] D. V. Matyushov and R. Schmid, The Journal of Chemical Physics **104**, 8627 (1996).
[15] All simulation temperatures were low enough such that atoms did not migrate across these artificial boundaries, as was determined by the absence of the corresponding step changes in the total energy.
[16] M. P. Allen and D. J. Tildesley, *Computer Simulation of Liquids* (Clarendon Press, Oxford, 1990).
[17] H. J. C. Berendsen, J. P. M. Postma, W. F. van Gunsteren, A. DiNola, and J. R. Haak, Journal of Chemical Physics **81**, 3684 (1984).
[18] D. S. Ivanov and L. V. Zhigilei, Physical Review B **68**, 064114 (2003).
[19] J. C. Duda, T. S. English, D. A. Jordan, P. M. Norris, and W. A. Soffa, Journal of Physics: Condensed Matter **23** (2011).
[20] J. C. Duda, P. M. Norris, and P. E. Hopkins, Journal of Heat Transfer **133**, 074501 (2011).
[21] C. F. Carlborg, J. Shiomi, and S. Maruyama, Physical Review B **78**, 205406 (2008).
[22] N. Shenogina, P. Keblinski, and S. Garde, The Journal of Chemical Physics **129**, 155105 (2008).